Shaft Capacity of Open-Ended Piles in Sand

David John Paul Igoe[1]; Kenneth George Gavin[2]; and Brendan C. O'Kelly[3]

Abstract: This paper presents the results from an experimental investigation designed to examine the effect of soil-core development and cyclic loading on the shaft resistance developed by open-ended piles in sand. An instrumented open-ended model pile was installed either by driving or jacking into an artificially-created loose sand deposit in Blessington, Ireland. The tests provided continuous measurements of the soil-core development and the radial effective stresses during installation and subsequent load tests. The equalized radial effective stresses developed at the pile-soil interface were seen to be dependent on the degree of soil displacement (plugging) experienced during installation, the distance from the pile toe, and the number of load cycles experienced by a soil element adjacent to the pile shaft. A new design method for estimating the shaft capacity of piles in sand is proposed and compared with measurements made on prototype field-scale piles. **DOI: 10.1061/(ASCE)GT.1943-5606.0000511.**

CE Database subject headings: Piles; Shafts; Cyclic loads; Sand (soil type).

Author keywords: Open-ended piles; Shaft capacity; Plugging; Cyclic loading.

Background

The industry standard method for the design of offshore open-ended piles in sand is the American Petroleum Institute (API; 2006) RP2A approach. The method calculates the unit shaft friction mobilized during failure (τ_f) at a given depth by using an effective stress approach

$$\tau_f = \beta \sigma'_{v0} \tag{1}$$

where σ'_{v0} = in situ vertical effective stress; and β (a dimensionless factor) for unplugged piles varies from 0.29 for medium dense sand to 0.56 for very dense sand. The method differentiates between open- and closed-ended (or plugged) piles by applying a 25% higher β value to closed-ended piles. Despite receiving strong criticism because of its highly empirical nature and poor predictive reliability when tested against field test databases, this method has remained popular primarily because of its ease of application and long history of use. Research with both model and full-scale piles has illustrated the strong effect of sand density and stress level on the shaft friction mobilized by piles in sand. This has resulted in direct correlations between the average unit shaft friction (τ_{av}) and in situ tests such as the cone penetration test (CPT) end resistance (q_c)

$$\tau_{av} = \alpha q_c \tag{2}$$

Various workers have recommended α values, of which many are based on experience from onshore (often closed-ended) pile tests. Meyerhoff (1956) suggested α values of 0.005 for closed-ended piles and 0.0025 for low-displacement piles. Bustamante and Gianeselli (1982) suggested α ranges from 0.005 to 0.0017 depending on the type of pile, soil type, and magnitude of q_c, although they did not differentiate between open and closed-ended piles. On the basis of experience from offshore piling, De Ruiter and Beringen (1979) developed an approach in which $\alpha = 0.003$. Foye et al. (2009) suggested α increases from 0.002 for open-ended piles to 0.005 for closed-ended piles.

The preceding α and API methods make no explicit allowance for the effects of friction fatigue, which was defined by Hereema (1980) as the reduction of the shear stress in a given soil layer during installation as the distance from the pile tip (h) increased. This is a well accepted feature of displacement pile behavior (Vesic 1970; Lehane and Jardine 1994; Randolph 2003) and has been incorporated in recent CPT-based design approaches (see Lehane et al. 2005; Jardine et al. 2005). Model pile tests performed with the closed-ended Imperial College Pile (ICP), reported by Lehane (1992) and Chow (1997), which allowed simultaneous measurement of radial effective stresses and local shear stress along the pile shaft have resulted in significant advances in our understanding of the mechanisms controlling the shaft resistance developed by piles in sand. These model pile tests confirmed that the shaft friction was controlled by the Mohr-Coulomb failure criterion relating the ultimate local unit shaft friction to the radial effective stress at failure, σ'_{rf}, and the interface friction angle, δ_f, in which

$$\tau_f = \sigma'_{rf} \tan \delta_f \tag{3a}$$

$$\sigma'_{rf} = \sigma'_{rc} + \Delta\sigma'_{rd} \tag{3b}$$

where σ'_{rc} = radial effective stress measured after installation but before loading; and σ'_{rd} = increase in radial effective stress that occurs owing to dilation during loading. Lehane and Jardine (1994) showed that σ'_{rd} values can be predicted by using cavity expansion theory [see Eq. (4)] and note that dilation effects can dominate the shaft friction mobilized on model piles

$$\Delta\sigma'_{rd} = 4G\left(\frac{\Delta r}{R}\right) \tag{4}$$

[1]Postdoctoral Researcher, School of Architecture, Landscape, and Civil Engineering, Univ. College Dublin, Newstead Building, Belfield, Dublin 4, Ireland (corresponding author). E-mail: david.igoe@ucd.ie

[2]Lecturer, School of Architecture, Landscape, and Civil Engineering, Univ. College Dublin, Newstead Building, Belfield, Dublin 4, Ireland. E-mail: kenneth.gavin@ucd.ie

[3]Senior Lecturer, Dept. of Civil, Structural, and Environmental Engineering, Trinity College Dublin, Ireland. E-mail: bokelly@tcd.ie

Note. This manuscript was submitted on November 24, 2009; approved on January 14, 2011; published online on January 18, 2011. Discussion period open until March 1, 2012; separate discussions must be submitted for individual papers. This paper is part of the ***Journal of Geotechnical and Geoenvironmental Engineering***, Vol. 137, No. 10, October 1, 2011. ©ASCE, ISSN 1090-0241/2011/10-903–913/$25.00.

where G = sand shear stiffness; Δr = interface dilation; and R = pile radius. Hence, the accurate determination of the capacity of full-scale piles depends on reliable estimates of σ'_{rc}. Tests performed with the ICP demonstrated that the equalized local radial effective stresses, σ'_{rc}, rose and fell synchronously with the CPT end bearing, q_c, and hence with the sand state and relative density. The tests, conducted in both medium-dense and dense sand sites, consistently showed a decrease in σ'_{rc} with distance from the pile tip (and therefore, allowed for the quantification of friction fatigue). Jardine et al. (2005) proposed the following equation for predicting σ'_{rc}, which has become known as the ICP-05 design method for closed-ended piles:

$$\sigma'_{rc} = \frac{q_c}{45}\left(\frac{h}{D}\right)^{-0.38}\left(\frac{\sigma'_{v0}}{P_{atm}}\right)^{0.13} \quad (5)$$

where h/D = distance from the pile tip normalized by pile diameter; and P_{atm} = atmospheric pressure (assumed at 100 kPa). In this expression, the constants in the first and second terms, which describe the ratio of radial effective stress to the q_c value mobilized near the toe of the pile and the effects of friction fatigue respectively, are independent of the sand state, whereas the third term suggests a weak stress dependence in the correlation. A number of researchers (e.g., Randolph 2003; White and Lehane 2004) have suggested that friction fatigue effects are controlled by the number of load cycles, N, experienced by the piles. Lehane et al. (2005) compiled a database of instrumented closed-ended pile tests and found that the following expression gave the best-fit to the available data:

$$\sigma'_{rc} = \frac{q_c}{33}\left(\frac{h}{D}\right)^{-0.5} \quad (6)$$

This expression, which is the basis for the University of Western Australia (UWA-05) design approach for estimating the shaft capacity of closed-ended piles in sand (Lehane et al. 2005), is shown in Fig. 1 to provide excellent estimates of the horizontal stress measurements made on the ICP at two test sites at Labenne (Lehane 1992) and Dunkirk (Chow 1997). Lehane et al. (2005) argue that the effects of cyclic degradation are included implicitly in Eq. (6) through the h/D term.

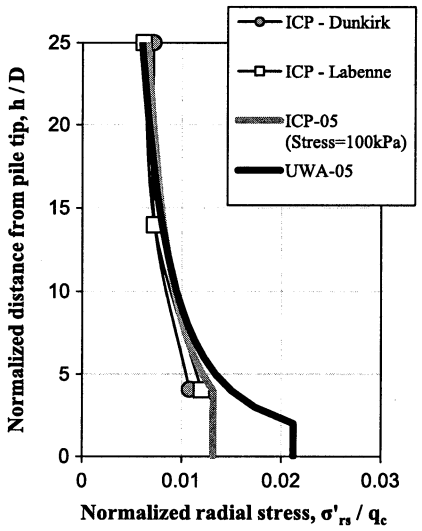

Fig. 1. Measured stationary radial effective stresses normalized by q_c at Dunkirk and Labenne compared with ICP-05 and UWA-05 design approaches

By measuring the radial effective stress response at the pile-soil interface, tests such as those performed by using the ICP have undoubtedly resulted in significant advances in our understanding of the mechanisms controlling the development of shaft friction on closed-ended piles. Although a number of model and prototype scale instrumented open-ended pile tests have been reported (e.g., Brucy et al. 1991; Paik and Lee 1993; Lehane and Gavin 2001; Lee et al. 2003), none have included radial stress measurements, which would improve the fundamental understanding of shaft friction developed by open-ended piles in a manner similar to the ICP pile tests. In the absence of such data, a number of empirical approaches have been proposed to modify expressions, such as Eqs. (5) and (6), to predict the radial effective stress developed by open-ended piles.

Chow (1997) considered how to adjust the σ'_{rc} values derived from Eq. (5) for closed-ended piles to account for the reduced levels of soil displacement and lower stress changes that occurred during the installation of an open-ended pile. This approach assumed the σ'_{rc} value developed near the toe of open and closed-ended piles was equal, and the rate of reduction of shear stress with h/D (friction fatigue term) was increased. This was achieved by substituting D in Eq. (5) with D^*

$$D^* = \sqrt{D^2 - D_i^2} \quad (7)$$

where D and D_i = external and internal diameters of the pile. This reduction technique, which implies that the pile remains fully coring throughout installation, was adopted in the ICP-05 design method.

White et al. (2005) argued that a stronger logical basis existed for applying a modification to the q_c term in Eq. (5), resulting in reduced shaft friction near the pile toe. It was argued that the degree of plugging experienced by open-ended piles should be taken into consideration. This may be defined by the incremental filling ratio (IFR)

$$\text{IFR} = \frac{\Delta L_p}{\Delta L} \quad (8)$$

where ΔL_p = change in the soil plug length during an increase in pile penetration ΔL. By using cavity expansion theory, White et al. (2005) argued for a scalar reduction factor in the form of an effective area ratio $A_{r,\text{eff}}$

$$A_{r,\text{eff}} = 1 - \text{IFR}\left(\frac{D_i}{D}\right)^2 \quad (9)$$

where $A_{r,\text{eff}}$ expressed as a power law is used to modify the UWA design method for closed-ended piles [given in Eq. (6)] to account for open-ended conditions

$$\sigma'_{rc} = \frac{q_c}{33}A_{r,\text{eff}}^{0.3}\left(\frac{h}{D}\right)^{-0.5} \quad (10)$$

In the absence of a measured IFR profile, Lehane et al. 2005 proposed a simple empirical correlation for predicting IFR at the end of installation as follows:

$$\text{IFR} = \max\left[\left(\frac{D_i}{1.5}\right)^{0.2}, 1\right] \quad (11)$$

Given the uncertainties in the difference between the shaft resistance values developed by open- and closed-ended piles in sand, this paper describes the field tests performed with instrumented open- and closed-ended piles equipped with radial effective stress sensors located at multiple levels along the pile shaft. The radial

effective stresses mobilized during installation and cyclic load testing are discussed, and a new design method for estimating the shaft capacity of open-ended piles is proposed. Finally, the proposed design approach is used to calculate the shaft resistance mobilized by full-scale piles.

Experimental Details

Site Description

The pile tests were performed at the University College Dublin (UCD) test site situated in Blessington, 25 km southwest of Dublin city. The ground conditions at the site and the sand properties have been reported in Gavin and O'Kelly (2007) and Gavin et al. (2009) among others. In summary, the ground conditions are comprised of a very dense, glacially deposited fine sand with a relative density close to 100%, CPT q_c resistance in the range of 15–20 MPa, and a small strain stiffness (G_0) in the range 100–150 MPa. Particle size distribution analyses performed on samples taken from depths ranging from 0.7–2 m below ground level (BGL) indicated the mean particle size, D_{50}, varied between 0.1 and 0.15 mm (Fig. 2). The sand had a fines content (percentage of clay and silt particles) between 5 and 10%. Samples typically had less than 10% coarse grained particles (> 0.6 mm). The water table was approximately 13 m BGL. Considering the high CPT q_c values at the site, the instrumented model pile could not be installed in the naturally overconsolidated ground. To overcome this, a large 2.5-m-wide, 10-m-long, and 6–7-m-deep trench was excavated at the site. The excavated material was backfilled into the trench maintaining a minimum drop height of 1 m that resulted in the formation of a uniform deposit of loose sand.

Two weeks after the formation of the test bed, four CPTs were performed at 2 m spacings along the trench. Four additional CPT traces were performed six months after the trench formation to assess temporal variations in the sand state. The average CPT q_c and side friction (f_s) profiles for all 8 CPTs are shown in Fig. 3 (solid line). The range of CPT values are highlighted by the upper- and lower-bound profiles (dashed lines). The CPTs performed six months after the formation of the trench had significantly higher q_c values near the ground surface (up to ≈ 1.2 m depth) than those performed after 2 weeks. This was assumed to be attributable to trafficking of the area by both the CPT truck that performed the pile experiments in this period and general quarry traffic. Below 1.2 m, the CPT q_c and side friction (f_s) profiles were consistent at all locations in the trench. The q_c remained relatively steady at 0.8 to 1.0 MPa until the cone tip reached the base of the trench at 6–7 m BGL. The pile tests were performed between 2 weeks and 6 months of the formation of the trench and were all performed from the base of 0.85 to 1.9-m-deep starter holes because this was the required clearance to position the instrumented piles beneath the CPT truck. Hence, all the pile tests were essentially performed in the zone unaffected by trafficking.

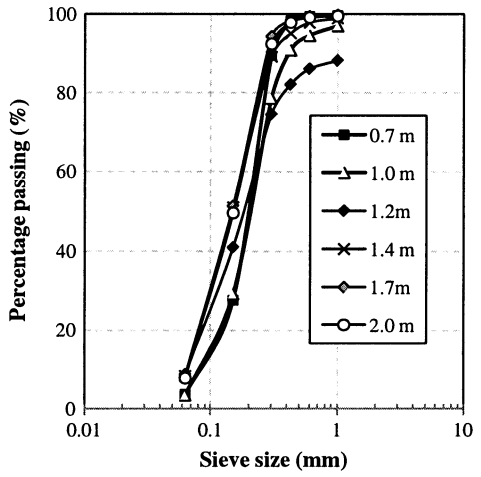

Fig. 2. Particle size distribution analysis on Blessington sand

Profiles of the small strain shear modulus, G_0, determined by multichannel analysis of surface waves (MASW) are shown in Fig. 3(c). The G_0 values in the trench increased from 20 MPa near the ground surface to ≈35 MPa at depth. Although these G_0 values are approximately 25–35% of those measured in the natural dense sand, the CPT q_c values in the trench are only 6–7% those recorded in the natural ground. Therefore, the excavate and replace process altered the ratio of G_0/q_c from ≈6 for the natural sand to ≈35 for the trench.

Model Piles

Model open- and closed-ended piles were used in the tests described in this paper. The stainless steel open-ended pile had an external diameter of 168 mm and a wall thickness (t) of 9 mm, giving a D/t ratio of 19 (which is within the D/t range of 15–45, noted by Jardine and Chow 2007, typical for offshore piles). The lower instrumented section, 2 m in length, was constructed by using the twin-walled technique in which two strain-gauged steel pipes with slightly different diameter are joined (at the top), thus allowing separate measurement of the internal and external shaft resistance and the base load developed on the annulus of the pile toe itself. Three instrumented units, which housed the radial total stress sensors and pore pressure transducers were located at h/D = 1.5, 5.5, and 10.5. Spacer sections machined from the same pipe that were 1.0 m in length and of equal diameter could be used to allow pile installation to 6 m. The stress sensors were TML (Tokyo Sokki Kenkyujo Co.) PDA-500 kPa and had a rated capacity of 500 kPa. The same sensors were used to measure pore pressure response (located diametrically opposite the total stress sensors). A porous ceramic disk was mounted flush with the outer pile surface in front of each of the pore pressure sensors. The location of the instrumentation, including the electrical resistance strain gauges are shown in Fig. 4. Full details of the design, construction, and calibration of the model pile are contained in Igoe et al. (2010a).

The model closed-ended pile used in the field tests was a 73-mm, stainless steel pile with radial total stress and pore-water pressure sensors at the same relative locations (h/D = 1.5, 5.5, and 10.5) as the open-ended piles and a similar level of overall instrumentation. This instrumentation is described in detail by Igoe (2010).

Test Program

The installation and load testing of three piles is described in this paper. The piles were installed through initial bore holes (with the bore wall supported by PVC tubing), and penetration continued until the piles approached the base of the trench (see Fig. 5). The first test (OE1) involved jacking the open-ended model pile into the ground at a rate of 20 mm/s and by using the CPT truck as a reaction. The pile was jacked from the bottom of a 1.9-m-deep starter hole to a final depth of 5.9 m BGL. The installation was paused and the pile head completely unloaded after each 100 mm of penetration to monitor the plug development and record the stationary radial effective stresses under a fixed number of jacking

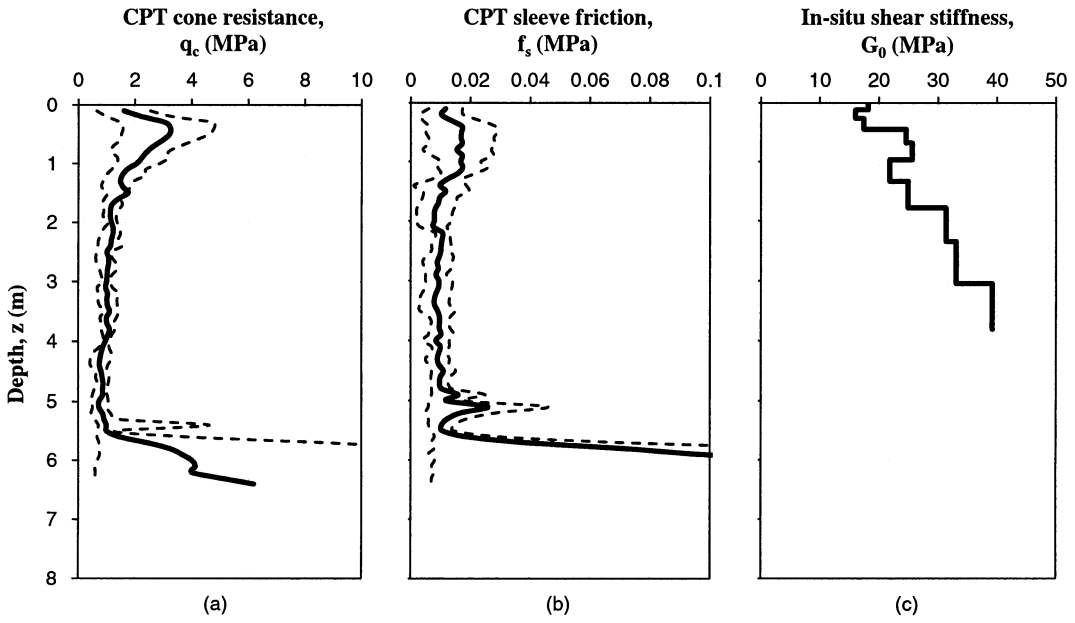

Fig. 3. (a) CPT end bearing q_c; (b) CPT sleeve friction f_s; and (c) in-situ shear stiffness G_o determined by MASW

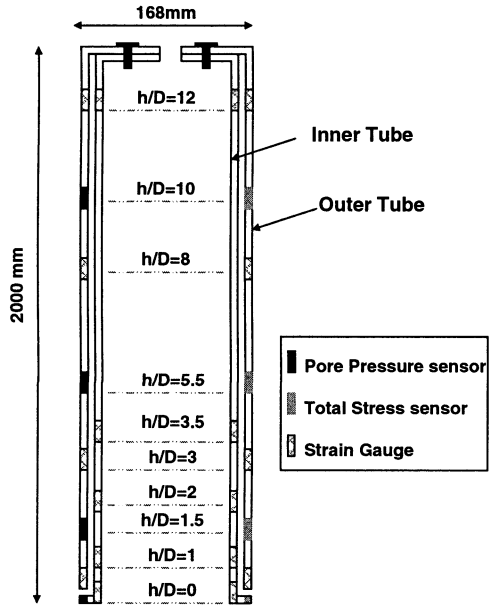

Fig. 4. UCD open-ended model pile instrumentation layout (after Igoe et al. 2010a)

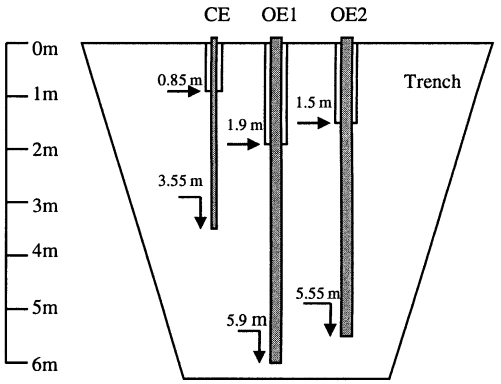

Fig. 5. Layout of the pile tests in the trench in Blessington

cycles. Some of the initial findings on the installation phase of pile OE1 were reported in Igoe et al. (2010a, b). The second test (OE2) involved driving the pile from a 1.5-m-deep starter hole to a depth of 4.1 m. Driving was achieved by using a 25 kg hammer allowed to free-fall vertically through a drop-height of 0.5 m. The hammer was machined from a solid 150-mm-diameter, mild steel shaft that had a hole drilled through its center to accommodate an alignment bar. The alignment bar was threaded into the pile cap, thus ensuring good contact between the hammer and pile during each blow. Driving was paused after each 100-mm penetration to allow plug and stress measurements to be recorded. Following a sequence of load tests (described in Table 1), the pile was pushed a further 1.4 m into the ground with the CPT truck with 50-mm jacking strokes. The final test involved the installation of the 73-mm-diameter closed-ended model pile that was installed with the CPT truck in 50-mm jacking strokes. The pile was jacked from a 0.85-m-deep starting hole to a final depth of 3.55 m after which a series of cyclic load tests were conducted.

Experimental Results

Plug Development

The IFR profiles measured during installation of the two open-ended piles are shown in Fig. 6. Pile OE1 remained fully coring (IFR = 100%) for only the first 100-mm jacking stroke. Thereafter, the pile experienced significant plugging and became fully plugged (IFR = 0%) after 11 jacking strokes corresponding to a pile embedment depth of 1.1 m. It remained fully plugged until the final

Table 1. Installation and Load Test Details from Blessington Trench

Test number	Description	Details	Comments
1	OE1	Jacked installation in 100 mm strokes	Starting depth = 1.9 m, final depth = 5.9 m
		Static compression load test	
		Static tension load test	
2	OE2 driving	Driven installation—884 blows	Starting depth = 1.5 m, end of driving = 4.1 m
		Static compression test	
		Cyclic test at 35 and 60%	
		Static compression test	
	OE2 jacking	Jacked installation in 50 mm strokes	Starting depth = 4.15 m, depth = 4.95 m,
		Cyclic compression test at 50%	final depth = 5.55 m
		Continued jacking in 50 mm strokes	
		Cyclic compression test at 35%	
		Static tension test	
3	CE	Jacked installation in 50 mm strokes test	Starting depth = 0.85 m, end of driving = 3.5 m
		Static compression	
		Cyclic test at 35 and 60%	

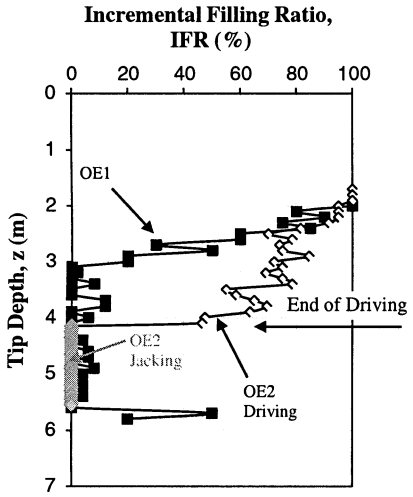

Fig. 6. IFR against pile toe depth

two jacking strokes, where the IFR value increased as the pile approached the bottom of the trench.

Pile OE2 remained partly coring with IFR reducing to ≈45% as it was driven over the depth range 1.5–4.1 m BGL. At this depth, a number of load tests were performed (see Table 1) during which time the pile remained fully plugged. The pile was subsequently jacked to a final penetration depth of 5.55 m BGL and remained fully plugged throughout.

Radial Effective Stresses

The three model pile tests presented in this study were conducted above the natural groundwater table, and hence, the pore-water pressures measured during testing were negligible. Because no radial stress changes were measured in the period between installation and load testing, the stationary radial effective stress, σ'_{rs} values measured when the piles were unloaded were therefore equivalent to the short- to medium-term equalized radial effective stresses ($\sigma'_{rs} = \sigma'_{rc}$). The values measured during installation of all three piles are shown in Fig. 7, and the following trends are noteworthy:

- The σ'_{rs} values measured during installation of the closed-ended pile [Fig. 7(a)] demonstrate that at a given h/D level, the σ'_{rs} profiles were relatively uniform with depth, albeit with a slight reduction evident between 2.2 and 2.8 m BGL. These profiles closely mirrored the CPT q_c profiles measured in this deposit. The effects of friction fatigue are obvious where σ'_{rs} decreased from 22–30 kPa at $h/D = 1.5$ to just 5–8 kPa at $h/D = 10.5$.
- The combined effects of pile plugging and friction fatigue on the σ'_{rs} values developed during the installation of a jacked open-ended pile OE1 (Igoe et al. 2010b) are demonstrated in Fig. 7(b), in which the σ'_{rs} values measured at $h/D = 1.5$ increased steadily as the sensor depth increased from 2–3 m BGL at the time when the pile moved from the fully coring to fully plugged mode of penetration. Both the measured σ'_{rs} values and the rate of increase in these values as the pile became plugged were much lower at $h/D = 5.5$.
- The effect of the number of load cycles and pile plugging on the σ'_{rs} values developed during the installation of an open-ended pile (OE2) are demonstrated in Fig. 7(c). During driven installation, in which the number of load cycles, N, exceeded 100, the σ'_{rs} values increased gradually with depth. Considering σ'_{rs} values recorded for pile toe depths of less than 3.25 m BGL (where IFR values were greater than 75%), similar radial stresses were measured at all sensor levels. Below this pile penetration depth, the IFR values reduced (to the range 45–68%) and the σ'_{rs} values near the pile tip (at $h/D = 1.5$) became higher than those measured elsewhere along the pile shaft. When the pile installation mode was changed to jacking at depths below 4.1 m BGL and the pile became fully plugged (IFR = 0%), the sensor at $h/D = 1.5$ registered a significant increase in the mobilized σ'_{rs} values. In contrast, neither of the other two sensors (at $h/D = 5.5$ and 10.5) registered increased radial stress, whereas the sensor at $10.5D$ remained within the depth range where the pile had been driven and the IFR value exceeded 45%. The sensor at $h/D = 5.5$ entered the depth range in which pile installation took place in the fully plugged condition. However, the performance of a cyclic load test when the pile toe depth was at 4.95 m BGL (sensor at 4 m BGL) meant the soil layer in which the sensor was measuring had experienced in excess of 100 load cycles.

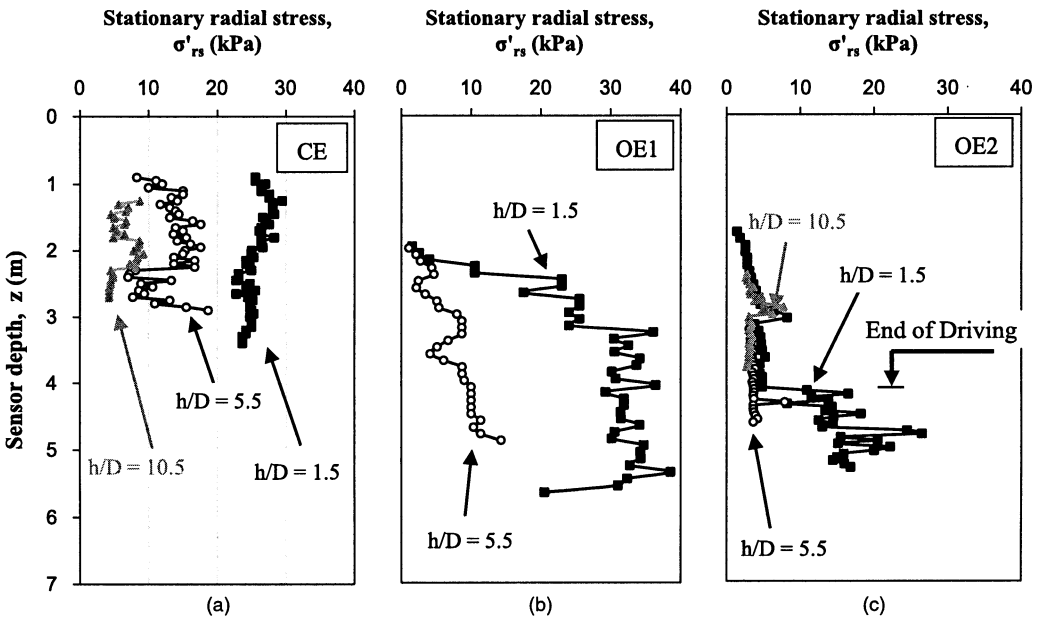

Fig. 7. Measured stationary radial effective stresses for (a) CE; (b) OE1; and (c) OE2

Discussion

Effect of Plugging

The field data suggest that σ'_{rs} values mobilized by open-ended piles depended on the CPT q_c resistance, the effect of soil plugging, h/D, and the number of load cycles experienced at the pile-soil interface. The effect of plugging is considered in Fig. 8 by plotting the normalized radial effective stress σ'_{rs}/q_c values measured during installation against IFR. Considering the sensor measurements at $h/D = 1.5$ [Fig. 8(a)], both piles mobilized similar increased minimum σ'_{rs}/q_c value of $\approx$0.003 when fully coring (IFR = 100%). As IFR decreased, both piles exhibited approximately linear increases in σ'_{rs}/q_c, although the rate at which this increase occurred was significantly different for the two piles considered. Pile OE1, which was installed by using 100 mm jacking strokes (causing three load cycles for each installation jacking stroke at $h/D = 1.5$), experienced a 10-fold increase in σ'_{rs}/q_c to $\approx$0.03 as IFR decreased from 100% to 0. Further increases in the ratio σ'_{rs}/q_c of approximately 33% occurred as the pile was jacked further in plugged mode (IFR = 0). During driven installation, pile OE2 experienced approximately 100 load cycles during every 100-mm penetration. The increase of σ'_{rs}/q_c measured during the driven installation of pile OE2, as IFR reduced from 100 to 45%, was significantly smaller than that measured on the jacked pile OE1. After driving, pile OE2 was jacked by using 50-mm strokes from 4.15–5.55 m BGL. The pile remained fully plugged (IFR = 0) throughout this installation stage and the σ'_{rs}/q_c ratio increased with depth to a maximum value of 0.033.

Considering the sensor measurements at $h/D = 5.5$ [Fig. 8(b)], both piles mobilized a similar minimum σ'_{rs}/q_c value of $\approx$0.003 when fully coring (IFR = 100%). The sensor on pile OE1, which was jacked into place, experienced nine installation load cycles, and the ratio σ'_{rs}/q_c increased linearly as IFR reduced, reaching a value of $\approx$0.008 when the pile first became plugged. This ratio increased substantially to $\approx$0.015 as the pile was jacked in the fully plugged condition. The sensor on pile OE2, which experienced more than 100 load cycles, mobilized similar σ'_{rs} values to the jacked pile when the IFR value was high (IFR > 50%). However, a much lower σ'_{rs}/q_c ratio of $\approx$0.005 was mobilized by this pile when it became fully plugged.

Considering the sensor measurements at $h/D = 10.5$ [Fig. 8(c)], the sensor on pile OE1 did not function during pile installation, and only data from the sensor on pile OE2 (that had experienced more than 100 installation load cycles) was available. The data show that a minimum σ'_{rs}/q_c value of $\approx$0.003 (comparable to the minimum recorded at all other sensor levels) was mobilized when IFR = 100%. Unlike the response noted at all other sensor levels, the ratio σ'_{rs}/q_c did not appear to increase as the IFR value at the sensor depth reduced to 55%.

Effect of Number of Load Cycles

The pile installation mode (number of installation load cycles experienced) had a significant effect on the radial effective stress developed. To investigate this effect further, the results of cyclic load tests performed on two piles; namely the closed-ended pile (CE1) and the open-ended pile (OE2) are compared in Fig. 9. In all the tests, one-way compression loading was applied with the load varied from 0 to 50–60% of the static axial capacity of the pile.

The cyclic load test on the closed-ended pile was performed at its final installation depth of 3.55 m BGL. The installation method of incremental jacking resulted in the application of a fixed number of installation load cycles at the sensor levels $h/D = 1.5$, 5.5, and 10.5. These are indicated by brackets in Fig. 9(a) in which (3) indicates that the sand at the sensor level $h/D = 1.5$ experienced three load cycles before the cyclic load test. A cyclic load test was performed on the open-ended pile at the end of driving (when the pile tip was at 4.1 m BGL), during the subsequent jacked installation stage (when the pile tip depth was at 4.95 m BGL), and again at the end of installation (5.55 m BGL). The variable installation method used for this pile meant that the ground at the level of the sensor at h/D of 1.5 experienced 100 installation load cycles before the cyclic test at 4.1 m BGL and only five load cycles before the tests at 4.95 m and 5.55 m BGL, respectively. The IFR values

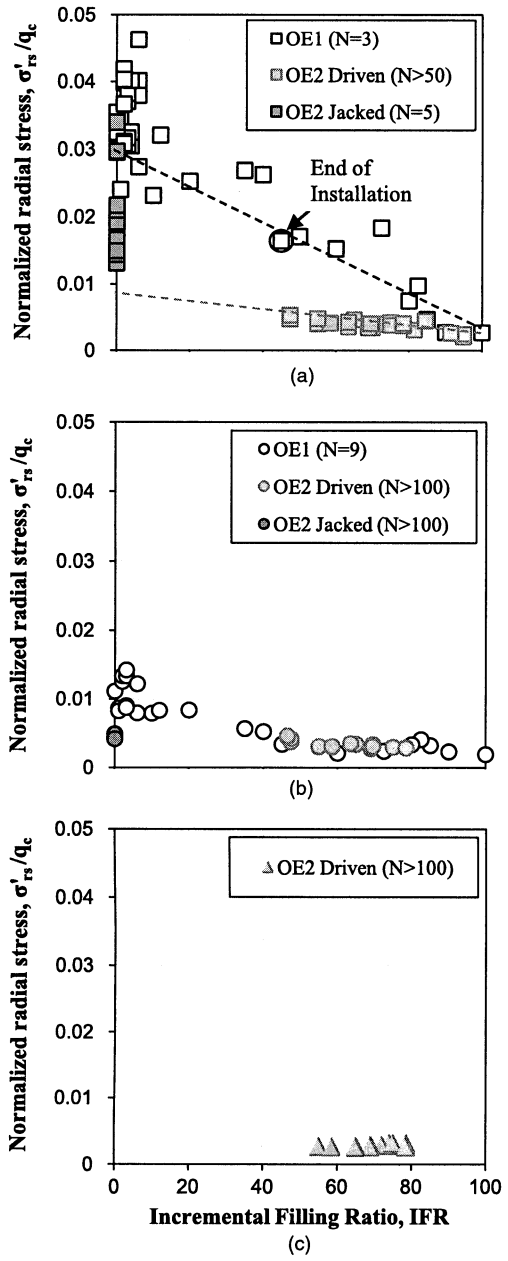

Fig. 8. IFR against normalized stationary radial stress at (a) $h/D = 1.5$; (b) $h/D = 5.5$; and (c) $h/D = 10.5$

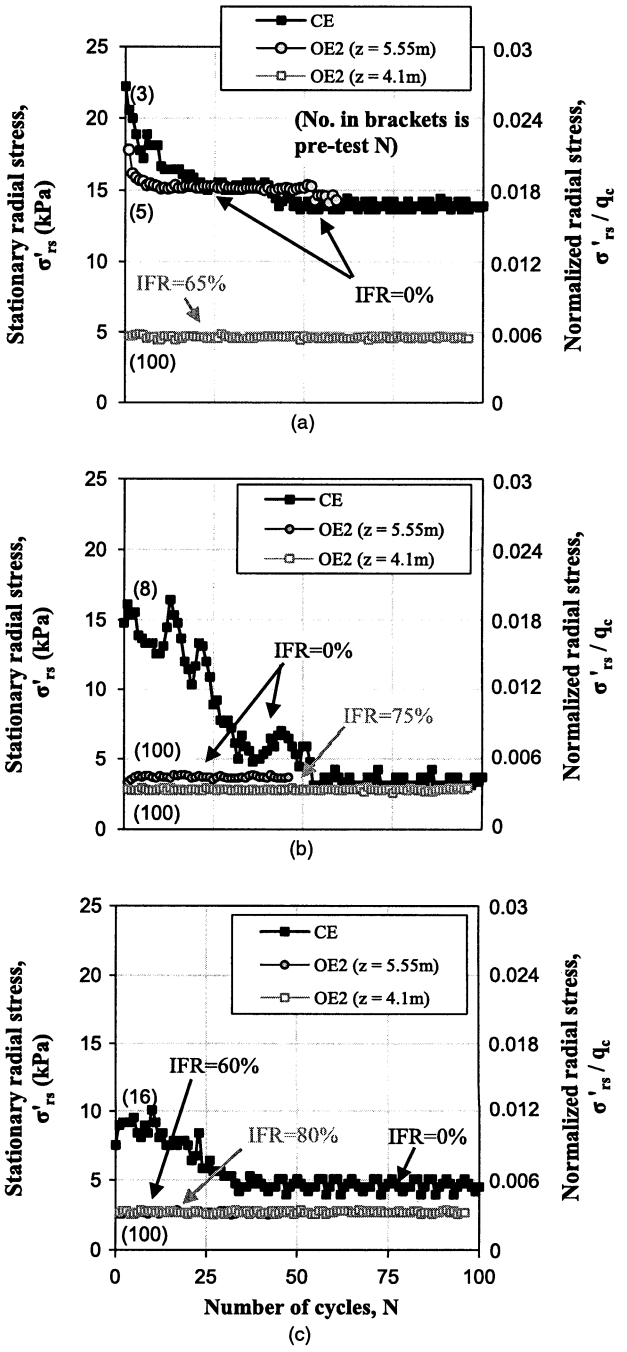

Fig. 9. Effect of cycling on stationary radial effective stresses at (a) $h/D = 1.5$; (b) $h/D = 5.5$; and (c) $h/D = 10.5$

recorded when the pile toe passed the various sensor levels is also indicated in the figure.

Considering the response of the sensors nearest the pile toe (at $h/D = 1.5$) in Fig. 9(a), it is clear that before the performance of the cyclic load test, σ'_{rs} values were highest on the two piles with the IFR values of 0%, and of these, σ'_{rs} was highest on the pile that had experienced the smallest number of installation load cycles. During the cyclic load test that followed, the σ'_{rs} values on these two piles decreased rapidly during the early part of the test to a minimum value of 14–15 kPa after the application of between 10 and 40 load cycles. In contrast, the much lower initial σ'_{rs} value of 5 kPa measured by the sensor nearest the toe of the driven pile (that had experienced approximately 100 load cycles during installation) with an IFR value of 65% did not exhibit any change during the application of an additional 100 load cycles.

Because of the performance of the intermediate cyclic load test during the jacked installation phase of pile OE2 (see Table 1), the remaining sensors on the open-ended pile, although encountering a range of installation IFR values, all experienced in excess of 100 load cycles. The measurements made on the closed-ended pile can, however, provide an insight into the response of a pile with IFR = 0 that has experienced a relatively small number of load cycles. Considering the data from the sensors at $h/D = 5.5$ in

Fig. 9(b), despite having very different IFR values, the open-ended piles mobilized very similar test σ'_{rs} values of $\approx$4 kPa that were unaffected by further load cycling. The initial σ'_{rs} of 16 kPa mobilized during installation of the closed-ended pile (that experienced eight installation load cycles) decreased rapidly during the cyclic load test, reaching a similar minimum value to the open-ended piles of 3–4 kPa after approximately 50 load cycles. This suggests that unlike the response measured at $h/D = 1.5$, at this h/D level a minimum radial stress developed after cyclic loading did not depend significantly on degree of soil plugging experienced during installation.

The sensors at $h/D = 10.5$ [Fig. 9(c)] show that after the application of approximately 40 load cycles, the minimum radial stress mobilized on all piles was approximately equal at 3 kPa, suggesting that the postcyclic loading σ'_{rs} value remote from the pile tip was independent of IFR.

The combined effects of pile plugging, cyclic loading, and h/D on the ratio σ'_{rs}/q_c is shown in Fig. 10, which summarizes the changes in σ'_{rs} during cyclic load tests on pile CE1 and OE2 (closed-ended and fully plugged, respectively, with IFR = 0%) and compares these with σ'_{rs}/q_c values measured during installation of OE2 when the pile was fully coring. The following behavior is observed:

- At all sensor locations, σ'_{rs} reduced to minimum values as the number of loading cycles experienced increased (with fewer than 50 load cycles being sufficient to effect this reduction).
- The minimum σ'_{rs} mobilized near the pile tip (at $h/D = 1.5$) was affected strongly by the IFR value, with much higher values developed by the fully plugged and closed-ended piles.
- The effect of IFR reduced significantly as h/D increased, with the postcyclic loading minimum σ'_{rs}/q_c values developed by the fully plugged and closed-ended piles being only slightly higher than the value measured on the fully coring pile (IFR = 100%) at $h/D = 5.5$. At $h/D = 10.5$, the σ'_{rs}/q_c values on all piles were equal, suggesting that the IFR value had no effect on the minimum σ'_{rs} value mobilized away from the pile tip.

A new model (referred to as UCD-11) for estimating the shaft resistance of piles driven in sand can be suggested on the basis of trends observed from the Blessington pile tests. The local shaft friction τ_f is given by

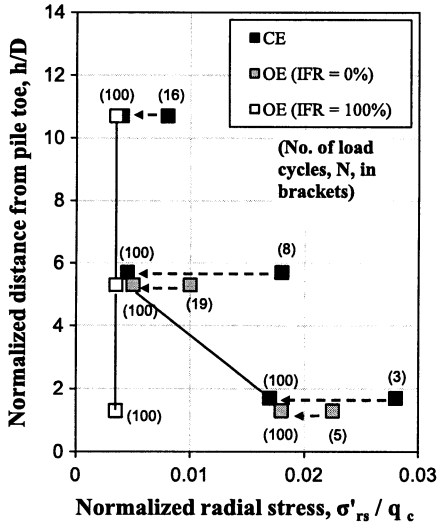

Fig. 10. Combined effect of cycling, plugging, and h/D on σ'_{rs}/q_c

$$\tau_f = (\sigma'_{rc} + \Delta\sigma'_{rd}) \tan \delta_f \quad (12a)$$

The radial effective stresses reduce from a maximum value at the pile toe (see Fig. 11), which is controlled by the q_c value and the degree of plugging experienced during installation, as quantified by the $A_{r,\text{eff}}$ value

$$\sigma'_{rc} = q_c[0.025 - 0.0025(h/D)]A_{r,\text{eff}} > \sigma'_{rc,\min} \quad (12b)$$

A linear reduction of radial effective stress occurs until the minimum radial effective stress $\sigma'_{rc,\min}$, which is unaffected by the degree of plugging, is developed

$$\sigma'_{rc,\min} = \lambda q_c \quad (12c)$$

where λ = scalar reduction factor that accounts for friction fatigue. Igoe (2010) investigated the effect of pile installation method on the radial effective stress developed by closed-ended piles installed in loose and very dense deposits of Blessington sand. Jacked-in-place piles that experienced a small number of load cycles developed similar normalized radial effective stress profiles in both the loose and dense deposits. However, when a large number of loading cycles were applied, the minimum normalized radial stresses were much lower in the loose sand deposit. It was argued that because volume reductions at the pile-soil interface control the reduction in radial effective stress during cyclic loading (see Randolph 2003), that friction fatigue effects should be dependent on the sand state with loose, compressible deposits exhibiting higher rates of friction fatigue in relation to the CPT q_c. Because of the limited data available, values of $\lambda = 0.003$ (for loose sand) and 0.006 (for dense sand) are proposed (Igoe 2010). Higher values may be possible in very dense sand deposits. The proposed design line for a range of $A_{r,\text{eff}}$ values from 0.2–1.0 in dense sand are shown in Fig. 11.

Application to Case Histories

The ability of the new design approach to predict the shaft resistance of large-scale instrumented piles installed in dense sand is compared with predictions made with both UWA-05 and ICP-05 in this section. Brucy et al. (1991) report load tests performed

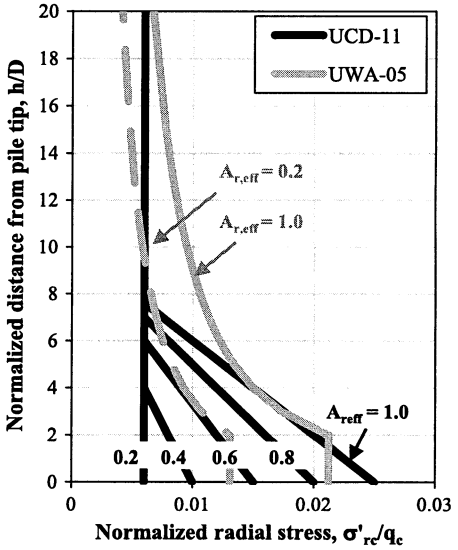

Fig. 11. New UCD-11 design approach compared with UWA-05 design method for a pile in dense sand

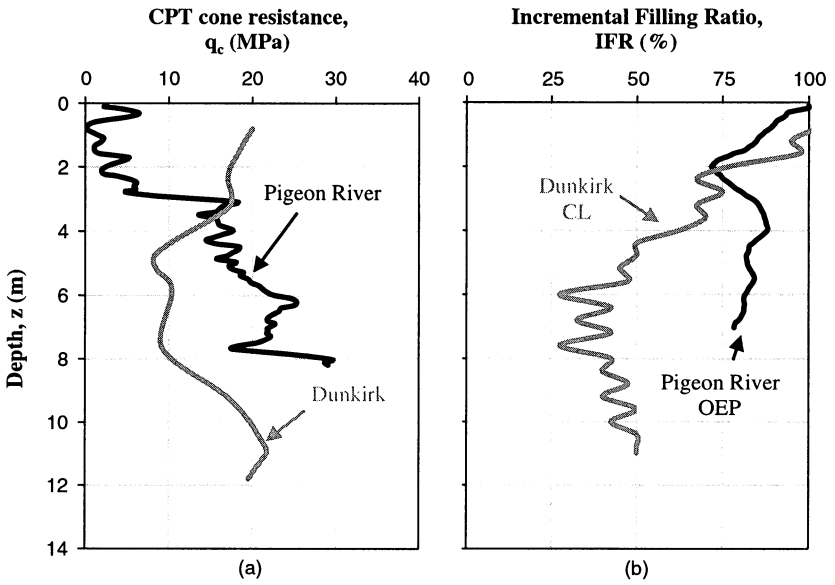

Fig. 12. (a) CPT q_c; and (b) IFR profiles from two case histories

on a 324-mm-diameter, 11-m-long, open-ended steel pile (pile CL) driven in dense sand at Dunkirk, northern France. The pile was instrumented with strain gauges at a number of levels, and Chow (1997) reported local shear stress distributions that were corrected for the effects of residual loads. Paik et al. (2003) describe load tests performed on a 356-mm-diameter, instrumented twin-walled pile (OEP) and a closed-ended pile of the same diameter (CEP), which were driven approximately 7 m through loose sand into a dense sand deposit at Pigeon River, Indiana. The CPT q_c profiles and IFR values measured at both sites are shown in Fig. 12.

Estimates of τ_f determined by using the three design approaches are shown in Fig. 13. Eq. (4) was used to provide estimates of dilation for the UCD-11 method and interface friction angles of 27° (Chow 1997) and 22.2° (Paik and Salgado 2003) were used for Dunkirk and Pigeon River, respectively. Fig. 12 demonstrates the following:

- All methods provide reasonably good overall estimates of the total shaft resistance developed by the open-ended pile at Dunkirk with the ratio of predicted to measured resistance at 99% for ICP-05, 116% for UWA-05, and 102% for UCD-11. However, both the ICP-05 and UWA-05 methods tended to overpredict τ_f near the pile base and underestimated the resistance near ground level. The new method provided better predictions of the distribution of the shaft stress.
- Both the ICP-05 and UWA-05 methods significantly overpredicted the shaft resistance developed by the open-ended pile

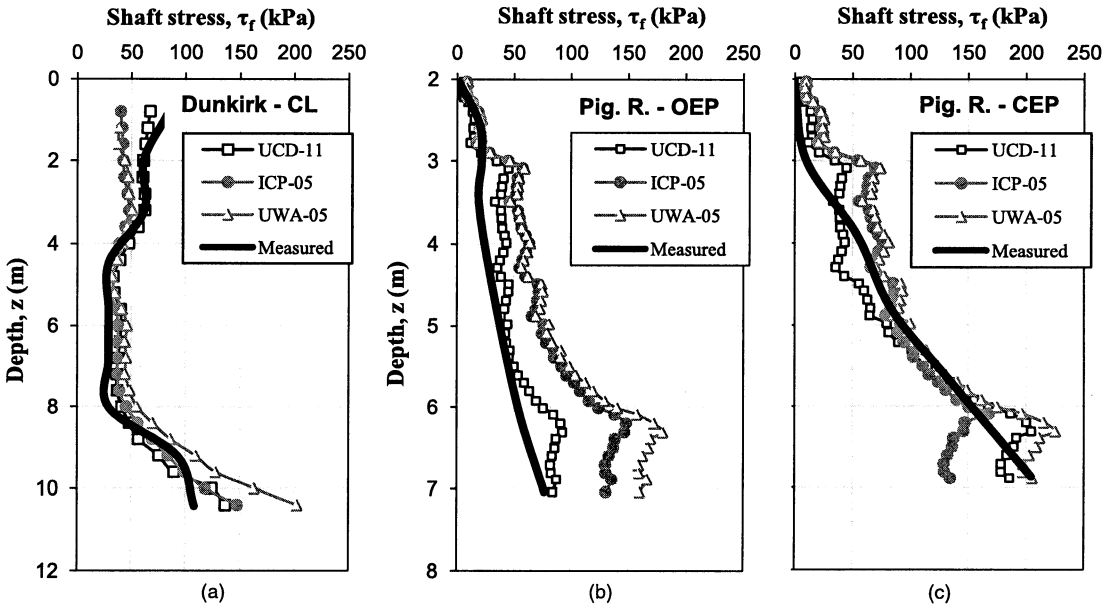

Fig. 13. Unit shaft friction profiles for (a) Dunkirk CL pile; (b) Pigeon River open-ended pile; and (c) Pigeon River closed-ended pile

installed at Pigeon River, with the two methods predicting 216 and 241% of the measured capacity, respectively. The predicted shear stress profiles clearly overestimated the τ_f values mobilized near the base of this pile, which had a high IFR throughout installation. The UCD-11 approach gave a much better overall prediction of the shaft resistance (with a ratio of predicted to measured shaft resistance of 134%) and again provided a good prediction of the distribution of the shaft stress. This particular case highlights the differences between the UCD-11 and the two other methods. The majority of the shaft resistance developed by this pile was mobilized within 10 diameters of the pile base. In contrast to the ICP-05 and UWA-05 design methods, UCD-11 suggests that piles which experience high IFR values during installation will not generate very large shear stresses near the pile tip.

- All methods provided relatively good predictions of the overall shaft resistance (with prediction to measured ratios of 117% for ICP-05, 141% for UWA-05, and 113% for UCD-11, respectively) and distribution of shear stress along the closed-ended pile installed at Pigeon River.

Conclusions

Tests conducted with the UCD instrumented open-ended model pile have provided reliable measurements of the radial effective stresses developed by piles installed in sand. The fully equalized radial effective stress σ'_{rc} acting on the external shaft of an open-ended pile was shown to depend on the number of load cycles, N, experienced by the soil horizon, the normalized distance from the pile tip, h/D, and the degree of plugging experienced during installation defined by using the IFR or $A_{r,\text{eff}}$ values. Approximately 50 loading cycles were sufficient to mobilize a minimum radial effective stress at the pile-soil interface. This minimum value was controlled by the CPT q_c value, h/D, and the degree of plugging experienced during installation only in a zone within 5–8 pile diameters from the base of the pile. Above this level, the minimum radial stress was a constant function of the CPT q_c value only. A simple design approach was proposed to estimate the shaft resistance of piles in sand. This provided better estimates of both the total shaft resistance and distribution of local shear stress developed on full-scale piles reported in the literature.

Publisher's Note. This paper was posted ahead of print with an incomplete author list. The complete author list appears in this version of the paper.

Acknowledgments

The authors would like to thank the following:

1. The first author was partly funded by an RPS-MCOS Scholarship and was a recipient of the Geotechnical Research Award from the Institute of Engineers Ireland (IEI);
2. Dave McAuley and Martin Carney for performing the CPT tests and in assisting with the pile installation and load testing at the Blessington site;
3. The Department of Civil, Structural, and Environmental Engineering, Trinity College Dublin, for the use of the TCD CPT truck; and
4. Roadstone Ltd., for access to the Blessington test site.

Notation

The following symbols are used in this paper:

$A_{r,\text{eff}}$ = effective area ratio;
D = external pile diameter (m);
D_i = internal pile diameter (m);
D^* = equivalent pile diameter (m);
f_s = CPT sleeve friction (Pa);
G = soil shear stiffness (Pa);
G_0 = small strain soil shear stiffness (Pa);
h = distance from pile toe (m);
K = coefficient of horizontal earth pressure;
L = pile length (m);
ΔL_p = change in plug length (m);
ΔL = change in pile penetration (m);
N = number of load cycles;
P_{atm} = atmospheric pressure = 100 kPa;
q_c = CPT cone resistance (Pa);
R = pile radius (m);
R_i = internal pile radius (m);
Δr = interface dilation (m);
t = pile wall thickness (m);
α = scalar CPT coefficient = τ_{av}/q_c;
β = $K \tan\delta_f = \tau_f/\sigma'_{v0}$;
λ = $\sigma'_{rc,\text{min}}/q_c$;
$\Delta\sigma'_{rd}$ = increase in radial effective stress during loading (Pa);
δ_f = interface friction angle at failure;
σ'_r = radial effective stress (Pa);
σ'_{rc} = equalized radial effective stress (Pa);
$\sigma'_{rc,\text{min}}$ = minimum equalized radial effective stress (Pa);
σ'_{rf} = peak radial effective stress at failure (Pa);
σ'_{rs} = stationary radial effective stress (Pa);
σ'_{v0} = in situ vertical effective stress (Pa);
τ_f = external unit shaft friction at failure (Pa); and
τ_{av} = average external unit shaft friction (Pa).

References

American Petroleum Institute (API). (2006). "Recommended practice for planning, designing and constructing fixed offshore platforms—Working stress design." *API RP2A*, API, Washington, DC.

Brucy, F., Meunier, K., and Nauroy, J. F. (1991). "Behavior of pile plug in sandy soils during and after driving." *Proc., Offshore Technology Conf.*, Richardson, TX, 145–154.

Bustamante, M., and Gianeselli, L. (1982). "Pile bearing capacity by means of static penetrometer CPT." *2nd European Symp. on Penetration Testing*, Amsterdam, 493–500.

Chow, F. C. (1997). "Investigations into behaviour of displacement piles for offshore structures." Ph.D. thesis, Civil Engineering Dept., Univ. of London (Imperial College), London.

De Ruiter, J., and Beringen, F. L. (1979). "Pile foundation for large North Sea structures." *Marine Geotechnol.*, 3(3), 267–314.

Foye, K. C., Abou-Jaoude, G., Prezzi, M., and Salgado, R. (2009). "Resistance factors for use in load and resistance factor design of driven pipe piles in sands." *J. Geotech. Geoenviron. Eng.*, 135(1), 1–13.

Gavin, K. G., Adekunte, A., and O'Kelly, B. C. (2009). "A field investigation of vertical footing response on sand." *Proc., Inst. Civ. Eng. Geotech. Eng.*, 162(5), 257–267.

Gavin, K. G., and O'Kelly, B. C. (2007). "Effect of friction fatigue on pile capacity in dense sand." *J. Geotech. Geoenviron. Eng.*, 133(1).

Hereema, E. P. (1980). "Predicting pile driveability: Heather as an illustration of the friction fatigue theory." *Ground Eng.*, 13, 15–37.

Igoe, D. (2010). "Offshore foundations: A comparison of full-displacement and partial-displacement piles in sand." Ph.D. thesis, School of Architecture, Landscape, and Civil Engineering, Univ. College Dublin (UCD), Ireland.

Igoe, D., Doherty, P., and Gavin, K. G. (2010a). "The development and testing of an instrumented open-ended model pile." *Geotech. Test. J.*, 33(1), 1–11.

Igoe, D., Gavin, K. G., and O'Kelly, B. C. (2010b). "Field tests using an instrumented model pipe pile in sand." *Proc., 7th Int. Conf. on Physical Modelling in Geotechnics*, Zurich, Switzerland, 775–780.

Jardine, R. J., and Chow, F. C. (2007). "Some recent developments in offshore pile design." *6th Int. Offshore Site Investigation and Geotechnics Conf.*, London.

Jardine, R. J., Chow, F. C., Overy, R. F., and Standing, J. R. (2005). *ICP design methods for driven piles in sands and clays*, T. Telford, ed., Univ. of London (Imperial College), London.

Lee, J. H., Salgado, R., and Paik, K. H. (2003). "Estimation of load capacity of pipe piles in sand based on cone penetration test results." *J. Geotech. Geoenviron. Eng.*, 129(5), 391–403.

Lehane, B. M. (1992). "Experimental investigations of pile behaviour using instrumented field piles." Ph.D. thesis, Civil Engineering Dept., Univ. of London (Imperial College), London.

Lehane, B. M., and Gavin, K. G. (2001). "Base resistance of jacked pipe piles in sand." *J. Geotech. Geoenviron. Eng.*, 127(6), 473–479.

Lehane, B. M., and Jardine, R. J. (1994). "Shaft capacity of driven piles in sand: A new design approach." *Conf. on the Behaviour of Offshore Structures*, Boston, 23–36.

Lehane, B. M., Schneider, J. A., and Xu, X. (2005). "The UWA-05 method for prediction of axial capacity of driven piles in sand." *1st Int. Symp. on Frontiers in Offshore Geotechnics (ISFOG)*, Univ. of Western Australia, Perth, Australia, 683–689.

Meyerhoff, G. (1956). "Penetration tests and bearing capacity of cohesionless soils." *J. Soil Mech. and Found. Div.*, 82(1), 819–886.

Paik, K. H., and Lee, S. R. (1993). "Behaviour of soil plugs in open-ended model piles driven into sands." *Mar. Georesour. Geotechnol.*, 11(4), 353–373.

Paik, K. H., and Salgado, R. (2003). "Determination of bearing capacity of open-ended piles in sand." *J. Geotech. Geoenviron. Eng.*, 129(1), 46–57.

Paik, K. H., Salgado, R., Lee, J. H., and Kim, B. J. (2003). "Behaviour of open- and closed- ended piles driven into sands." *J. Geotech. Geoenviron. Eng.*, 129(4), 296–306.

Randolph, M. F. (2003). "Science and empericism in pile foundation design." *Geotechnique*, 53(10), 847–875.

Vesic, A. S. (1970). "Tests on instrumented piles, Ogeechee River site." *J. Soil Mech. and Found. Div.*, 96(2), 561–584.

White, D. J., and Lehane, B. M. (2004). "Friction fatigue on displacement piles in sand." *Geotechnique*, 54(10), 645–658.

White, D. J., Schneider, J. A., and Lehane, B. M. (2005). "The influence of effective area ratio on shaft friction of displacement piles in sand." *1st Int. Symp. on Frontiers in Offshore Geotechnics (ISFOG)*, Univ. of Western Australia, Perth, Australia.